PAPER

Tuning thermal conductance of CNT interface junction via stretching and atomic bonding

IOP Publishing Journal of Physics D: Applied Physics
J. Phys. D: Appl. Phys. **50** (2017) 475302 (9pp) https://doi.org/10.1088/1361-6463/aa8ff8

Tuning thermal conductance of CNT interface junction via stretching and atomic bonding

Dongmei Liao[1,2], Wen Chen[2], Jingchao Zhang[3] and Yanan Yue[1,2,4]

[1] State Laboratory of Hydraulic Machinery Transients, MOE, Wuhan University, Wuhan 430072, People's Republic of China
[2] School of Power and Mechanical Engineering, Wuhan University, Wuhan, Hubei 430072, People's Republic of China
[3] Holland Computing Center, University of Nebraska-Lincoln, Lincoln, NE 68588, United States of America

E-mail: yyue@whu.edu.cn

Received 9 July 2017, revised 26 September 2017
Accepted for publication 29 September 2017
Published 30 October 2017

Abstract

In this work, various effects of stretching and bonding strength on the thermal transport at CNT junctions are comprehensively studied by classical molecular dynamics (MD) simulations. The modeling is performed on a typical parallel-aligned junction formed by two single-walled (10, 10) CNTs. The overlap length is the first condition we studied and it is found that thermal conductance is significantly increased from 1.00 to 11.76 nW K^{-1} with overlap length from 0.982 to 6.877 nm. Surprisingly, the thermal conductance per unit overlap length is increased rather than a constant value. The van der Waals interaction in non-bonded CNTs has a positive correlation on thermal conductance, which means thermal conductance can be effectively enhanced by applied force in the inter-tube direction. In the axial direction, the applied force is an important condition to adjust thermal conductance at bonded junction. Results show that the thermal conductance for overlap length of 1.966 nm can be enhanced from 2.81 to 3.42 nW K^{-1} at the initial stage because of the combined squeezing force. However, as applied force approaches the breaking value, the atomic bonding at the junction is greatly weakened with a rapidly dropping thermal conductance from 3.42 to 1.88 nW K^{-1}.

Keywords: carbon nanotube, molecular dynamics, thermal conductance

(Some figures may appear in colour only in the online journal)

1. Introduction

Heat dissipation has been a bottleneck in micro/nano-electronic devices due to continually decreasing sizes. Carbon nanotubes (CNTs) are outstanding thermal conductors for their high axial thermal conductivities of ~10^3 W m^{-1} K^{-1} as reported in experimental [1] and simulation [2] studies. They attract great attention and are regarded as excellent candidates for thermal management in micro/nano-electronic devices. The CNT bulk materials and CNT composites rather than individual CNTs are commonly used in devices, while their thermal conductivities are much lower than that of individual CNTs [3–5]. It is noticed that thermal resistance at CNT junction and CNT-matrix interface is the major factor suppressing thermal performance in CNT bulk materials [6–10]. Therefore, the enhancement of thermal transport in CNT bulk materials and CNT composites can be achieved by facilitating thermal coupling at CNT junction and CNT-matrix interface. The heat transfer mechanism at CNTs junction needs to be comprehensively studied [11].

There have been several works about thermal transport at CNT junctions by simulations [12–14] and experiments [15]. Hu *et al* [12] investigated the effects of CNT length, junction area and gas pressure on thermal conductance. It was found that

[4] Author to whom any correspondence should be addressed.

thermal conductance was increased with increasing CNT length and converged to 40 pW K^{-1}. It is increased with junction area while decreased with crossing angle. Hu *et al* [13] considered the effects of the crossing angle, nanotube length, and initial nanotube spacing on the thermal conductance at crossed CNTs junction. The results suggested that the thermal conductance was decreased with crossing angle and CNTs spacing, while increased with the nanotube length. Varshney *et al* [14] studied the effects of number and length of organic linkers connecting two parallel CNTs embedded in epoxy matrix on thermal conductance. It was reported that linker molecules significantly improved thermal transport, and thermal conductance had a positive dependence on the number of linkers while an inverse dependence on the length of linkers. Yang *et al* [15] measured the thermal conductance values of 10^{-8} W K^{-1} at cross junction between two CNTs with diameters of 74 and 121 nm and 10^{-6} W K^{-1} at aligned junction of 2.5 μm long between two CNTs with diameters of 170 and 165–185 nm. Aligned contact of CNTs junction with overlap segments is very common in CNTs fiber. The thermal conductance between CNTs has been reported in a few works [16–19]. It is found that the thermal conductance was increased as the overlap length was increased [16–19], and it was explained that more atoms contributed to the thermal transport with longer overlap length, which leads to enhanced thermal conductance. However, the dependence of thermal conductance per unit overlap length on overlap length was varied [16–19].

Mechanical stretching and squeezing by external force are alternative methods to manipulate thermal property of CNTs fiber [20]. Evans *et al* [21] investigated the effect of pressure on thermal conductance at the junctions of crossing angles 0° and 90°. The results show that thermal conductance was increased with pressure and was saturated at high pressure for different cases. Chen *et al* [22] considered the effects of internal coupling strength and external force on thermal conductance between cross-aligned CNTs. It was found that the thermal conductance was increased with increasing external force, and internal coupling strength, and external applied force shows similar effects on the thermal conductance. Liu *et al* [23] improved the thermal conductivity of silkworm silk from 0.54–6.53 to 13.1 W m^{-1} K^{-1} by mechanically stretching the silkworm silk with elongation of 68.3%. Yue *et al* [24] reported that thermal conductivity of CNTs fiber was increased as high as 28% with applied mechanical stretching less than 5% in the axial direction. Although the thermal conductance at CNTs junction has been explored extensively, the effect of applied force on thermal conductance needs to be further investigated to comprehensively understand the thermal transport mechanism. In this work, the thermal conductance is studied for the effect of various nanotube overlap lengths of bonded CNTs, non-bonded CNTs and applied external force in axial direction by MD simulations [25].

2. Computational details

The non-equilibrium molecular dynamics (NEMD) method [26] is used to investigate the thermal transport at aligned CNTs junction. As shown in figure 1(a), the atomic configuration

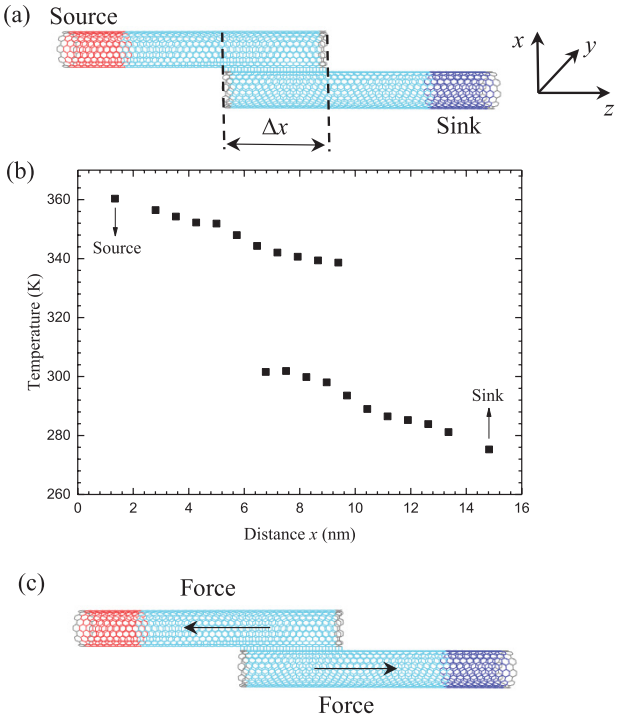

Figure 1. (a) The schematic structure for two parallel-aligned CNTs with covalent bonds and the overlap length is 3.934 nm (Δx). Free boundary conditions are used in all directions. (b) The temperature profiles of two bonded CNTs for overlap length of 3.934 nm. (c) The schematic structure for two parallel-aligned CNTs with covalent bonds and the overlap length is 3.934 nm. The black arrows represent applied force on CNTs. The gray regions represent carbon atoms which are fixed in the x and y directions, that is, the velocities of carbon atoms of outmost rings are always set as 0 in the x and y directions, but the velocity in the z direction of these atoms is not set.

modeling for the system consists of two 10 nm length CNTs with (10, 10) chirality. One end of CNT as shown as red region in figure 1(a) are selected as a hot source by adding a heat flux q, and one end of the other CNT as shown as blue region are regarded as the cold source by subtracting an equivalent heat flux q. The amount of thermal energy added to the hot source is equivalent to that subtracted from the cold source. Besides, 40 carbon atoms at each end of both CNTs as shown as gray regions in figure 1(a) are fixed to prevent the CNTs from rotating, which is conducted by setting the velocities of carbon atoms as 0 in all directions. The remaining region of each CNT is divided into 10 slabs along the transverse direction to obtain the temperature profile of the system. The temperature of each slab is calculated as

$$T = \frac{1}{3nk_{\mathrm{B}}} \sum_{k=1}^{n} m_k {v_k}^2 \qquad (1)$$

where n is the number of atoms in each slab, k_{B} is the Boltzmann constant, m_k and v_k are the atomic mass and velocity of atom k, respectively. The heat flux q and temperature drop ΔT at the junction calculated from the average temperatures of overlapping CNT segments can be used to calculate thermal conductance. The adaptive intermolecular reactive empirical bond-order (AIREBO) potential [27] is used. In more detail,

the 2nd generation REBO potential is used to describe carbon atomic interactions within CNTs, and the 12-6 Lennard Jones (LJ) [28] potential with parameters $\varepsilon = 2.84$ meV and $\sigma = 3.4$ Å is adopted to model the van der Waals interaction between CNTs. Different values of σ have been adopted in previous literatures. Xu *et al* [17] used van der Waals diameter $\sigma = 3.851$ Å for the LJ potential in a very early work. Later, Evans *et al* [21] and Hu *et al* [12] simulated the CNTs junctions with van der Waals interaction using the value of 3.4 Å. Considering our structure is similar to the above two works, the value of 3.4 Å is used in our simulations. The AIREBO potential E is described as

$$E = \frac{1}{2}\sum_{i}\sum_{j\neq i}[E_{ij}^{\mathrm{REBO}} + E_{ij}^{\mathrm{LJ}} + \sum_{k\neq i,j}\sum_{l\neq i,j,k} E_{kijl}^{\mathrm{TORSION}}] \quad (2)$$

where the E^{REBO} term describes short-ranged C–C, H–H and C–H interactions; the E^{LJ} describes long-ranged interactions and the E^{TORSION} term is an explicit 4-body potential that describes various dihedral angle preferences in hydrocarbon configurations, while the 12-6 Lennard Jones (LJ) potential V is expressed as [29]

$$V(r) = 4\chi\varepsilon\left[\left(\frac{\sigma}{r}\right)^{12} - \left(\frac{\sigma}{r}\right)^{6}\right] \quad (3)$$

where r is the interatomic distance; ε is the energy parameter, and σ is the van der Waals diameter. The scaling parameter χ is used to adjust the interaction strength between CNTs, which is discussed in detail for the effect of van der Waals interaction strength on thermal conductance.

The atomic configuration of overlap length of 3.934 nm between aligned CNTs is shown in figure 1(a). There are covalent bonds between CNTs. Usually, non-bonded CNTs junction is considered in most cases between CNTs. Currently, it is impossible to experimentally observe and validate such bonded interaction. However, the bonded structure has been considered in MD simulation. Shi *et al* [30] investigated the thermal transport in 3D carbon nanotube-graphene structure by molecular dynamics simulations and there was bonded interaction between carbon nanotube-graphene junctions. The system is initially equilibrated at temperature 300 K for 200 ps (1 ps = 10^{-12} s) using a Nose–Hoover thermostat [31] with an integration step of 0.2 fs (1 fs = 10^{-15} s). A consecutive micro-canonical ensemble (NVE) is followed for another 200 ps. Finally, a constant heat flux q is applied to the system for another 1.2 ns to reach steady state. The temperature is collected in the last 400 ps with temperature profiles as shown in figure 1(b).

A moderate temperature drop at the junction is important for thermal conductance calculation considering that larger temperature drop could induce non-linear effect, while lower temperature drop would lead to statistical uncertainties due to temperature fluctuation [21]. The heat fluxes applied in the study of effect of overlap length on thermal conductance are varied from 80 nW to 560 nW for overlap length from 0.982 nm to 6.886 nm to obtain ~50 K temperature drop at junction. The atomic configuration of studying the effect of applied external force on thermal conductance is shown in figure 1(c). The rings at the edge of carbon atoms marked as gray regions in figure 1(c) are fixed in the x and y directions, that is, the velocities of these carbon atoms are set as 0 in the x and y directions, but the velocity in the z direction of these atoms is not fixed. This setup is to ensure that CNTs would not rotate. The applied force in the z direction, as shown as the black arrows in figure 1(c), is applied in the axial direction to both CNTs.

3. Results and discussion

3.1. Thermal conductance calculation with various overlap length

The computational setup used in the simulation for overlap length of 3.934 nm is shown in figure 1(a). Free boundary conditions are used in all directions. The overlap length Δx as shown in figure 1(a) is varied from 0.982 nm to 6.877 nm, and the values of overlap length are carefully calculated for perfect alignment of two CNTs. According to the Fourier's law, the value of thermal conductance between CNTs is calculated as $G = q/\Delta T$, where q is heat flux and ΔT is the temperature drop at the CNTs junction. Figure 2(a) displays the thermal conductance G as a function of overlap length Δx. It is found that G is increased from 1.00 to 11.76 nW K^{-1} as Δx is increased from 0.982 to 6.877 nm. With larger overlap length Δx, more carbon atoms from both CNTs at the junction are involved and contribute to the thermal transport across the junction, which directly enhances the thermal conductance G. Moreover, it was reported that the CNTs length also have a strong effect on the interfacial thermal conductance at non-bonded junction [12]. Besides, it is found from literatures that CNTs length also has a certain effect on the intertube thermal conductance at bonded junction. For example, Yang *et al* [32] investigated the inter-tube thermal conductance between two CNTs and found the inter-tube conductance varied from 1.46×10^{-8} W K^{-1} to 1.64×10^{-8} W K^{-1} with the tube length ranging from 24.56 nm to 123 nm.

The thermal conductance per unit overlap length is defined as $\sigma = G/\Delta x$, and σ as a function of Δx is shown in figure 2(b). It is found that σ is increased with overlap length Δx. Richard *et al* [18] reported that thermal conductance per unit overlap length between two non-bonded CNTs with periodic boundary conditions had an inverted dependence on overlap length varied from 10 nm to 40 nm with CNT length of 100 nm. Volkov *et al* [16] found that the inter-tube conductance per unit length was independent on the overlap length varied from 0 to 100 nm. Xu *et al* [17] found that the dependence of thermal conductivity on overlap length was almost linear with overlap length varied from 0 to 10 nm, which indicated that thermal conductance per unit overlap length remained constant with overlap length. The tendency of thermal conductance per unit overlap length on overlap length in our work is different from that in other references. It is noticed that there are covalent bonds at the CNT junction in our work, thus the thermal conductance is mainly determined by the number of covalent bonds. The number of covalent bonds formed per unit length at the edge is small and lead to weaker thermal transport per unit length compared to the other region. The effect of edge

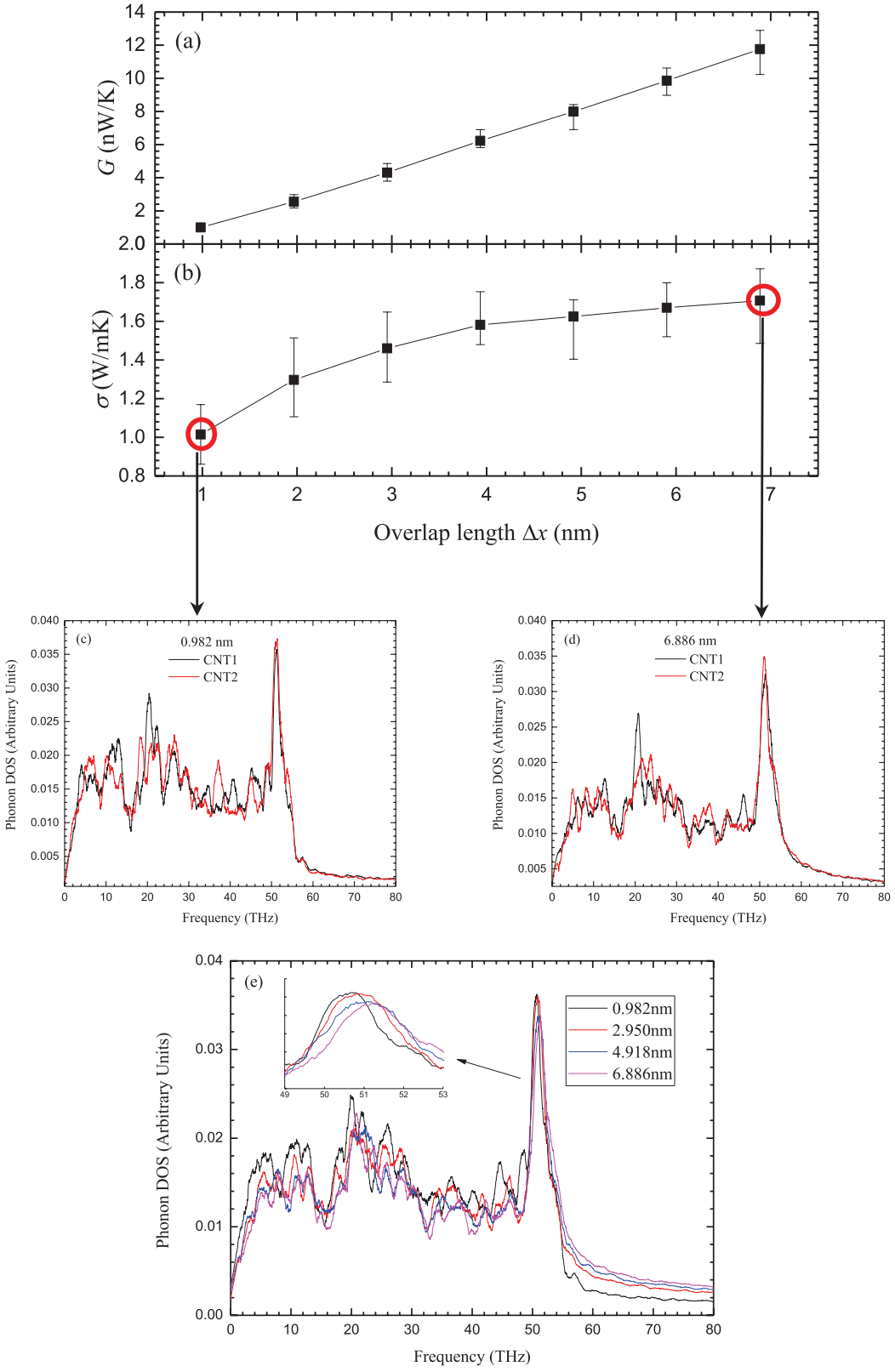

Figure 2. (a) Thermal conductance G as a function of overlap length Δx. (b) Thermal conductance per unit overlap length σ as a function of overlap length Δx. (c) The phonon DOS for overlap length of 0.982 nm. The red/black line denotes the phonon DOS for each side of CNT in overlap region. (d) The phonon DOS for overlap length of 6.886 nm. The red/black line denotes the phonon DOS for each side of CNT in overlap region. (e) The phonon DOS of CNTs on one side for overlap lengths of 0.982 nm, 2.950 nm, 4.918 nm and 6.886 nm. The inserted figure shows the shift of the phonon DOSs.

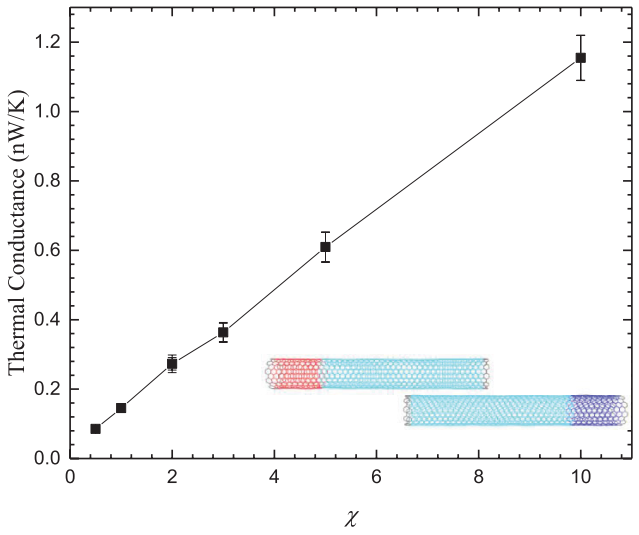

Figure 3. Thermal conductance G as a function of LJ scaling parameter χ. The inserted schematic structure displays two non-bonded CNTs with overlap length of 3.934 nm.

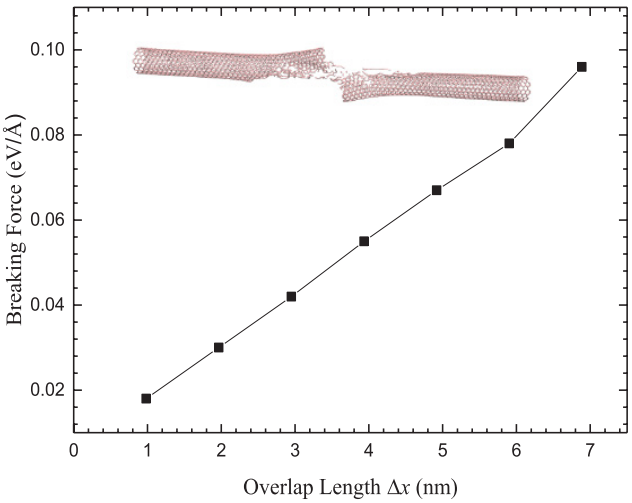

Figure 4. The breaking force, which is defined as the minimum force that can cut off the covalent bonds between CNTs and separate the two CNTs, as a function of overlap length Δx. The inserted schematic structure shows that the covalent bonds at the CNTs junction are cut off and the two CNTs are separated when the applied force is beyond breaking force.

on thermal conductance for shorter overlap length is more significant than that for longer overlap length since the ratio of edge region length on overlap length for longer overlap CNTs junction is smaller. Correspondingly, the thermal conductance per unit overlap length is increased with overlap length.

For quantitative analysis, the phonon DOS (density of states) curves for each CNT are drawn as shown in figures 2(c) and (d). The shortest overlap length 0.982 nm and longest overlap length 6.886 nm are selected for the analysis. Since there is not obvious distinction between these curves, the overlap area of the spectra is calculated to analyze the phonon scattering at interface. The overlap area of phonon DOS is defined as $\delta = \int A(f) f \mathrm{d}f$, where $A(f)$ is the intersected area at the frequency of f. It is calculated that the overlap area for these two cases are 32.7 and 40.4, respectively, partially explaining the increased thermal conductance per overlap length. Figure 2(e) was drawn to compare the phonon spectra of CNT on the same side for selected four different overlap lengths and found that the high frequency phonons exhibits a red shift with decreasing overlap length, which is similar to the previous reported observation about the softening of the G-band in the Raman spectra of single-layer graphene [33]. The phonon softening is able to reduce the phonon group velocity and relaxation time, which causes the reduction of thermal conductivity [34, 35]. The reduced phonon group velocities render less contribution from the phonon couplings to the interfacial heat flux, leading to lower inter-tube thermal conductance.

3.2. Effect of van der Waals interaction strength

The atomic configuration for studying the effect of van der Waals interaction strength on thermal conductance is shown as the inserted image in figure 3. The CNTs are interacted with van der Waals interaction, and the initial separation distance defined as the nearest distance between the outer walls of CNTs is 3 Å. Besides, the simulation process is the same as above-mentioned cases, while there is difference in heat flux value which is 0.8 nW in this case. Thermal conductance G for overlap length of 3.934 nm as a function of van der Waals interaction strength χ is shown in figure 3, which is implemented by tuning the scaling parameter χ in equation (3). As displayed in figure 3, the monotonic increasing dependence of G on χ indicates that the phonon coupling between two CNTs is enhanced with scale factor χ, which strengthens the thermal transport between two CNTs. The results indicate that thermal transport can be effectively manipulated by tuning the van der Waals interaction strength.

Although it is impossible to modify scaling parameter χ directly in practice, it can be achieved by applying external force or pressure [36], or through electron irradiation [37]. The dependence of thermal conductance between graphene sheets on interlayer interaction strength was investigated by Xu *et al* [17]. The tendency of thermal conductance on van der Waals interaction strength in the work by Xu *et al* is similar as that in our work. The thermal conductance G is 0.145 nW K^{-1} when $\chi = 1$, which is 0.35 nW K^{-1} for overlap length of about 4.2 nm for (10, 10) nanotubes in the work by Xu *et al* [17]. These results are comparable considering that larger energy parameter $\varepsilon = 0.004\,555$ eV for C–C in the work by Xu *et al* [17], while the value is 0.002 84 eV in our work. The thermal conductance of CNTs junction is 1.155 nW K^{-1} when χ is equal to 10, which is about 1.901 nW K^{-1} for graphene/graphene interface in Xu *et al*'s work [17]. Considering the difference in structure, the difference in thermal conductance is reasonable. Meanwhile, it is similar that thermal conductance is increased with LJ scaling parameter χ for both CNTs junction and graphene/graphene interface. It was reported that the thermal conductance for covalent bonded interface could be two orders of magnitude greater than that for van der Waals interaction interface [38]. The thermal conductance between two bonded CNTs for an overlap length of 3.934 nm is 6.224

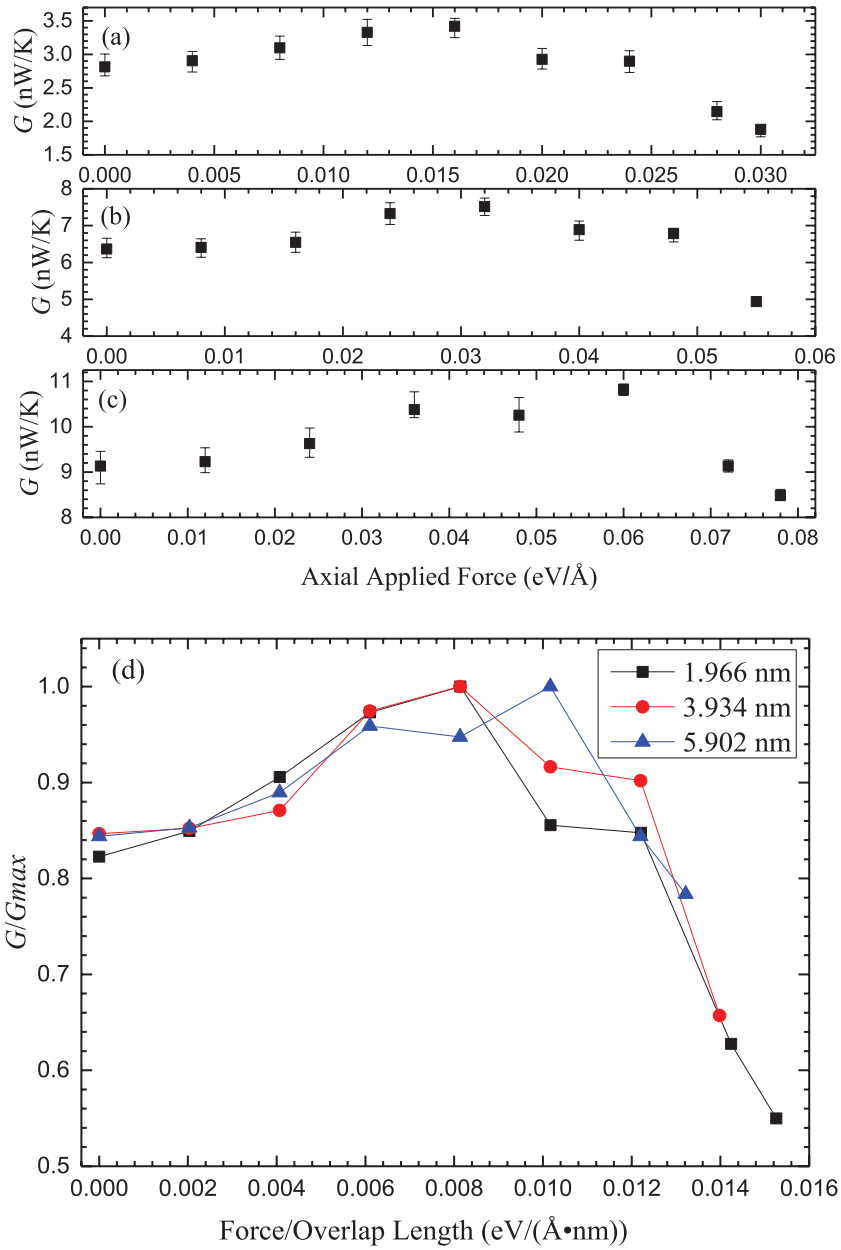

Figure 5. The relationship between thermal conductance G and applied force for overlap lengths of (a) 1.966 nm, (b) 3.934 nm and (c) 5.902 nm. (d) The relationships between normalized thermal conductance and normalized applied force.

nW K^{-1}, which is about 43 times larger than that for two non-bonded CNTs with the same overlap length in our work. Our results are reasonable compared with [17, 38].

3.3. Thermal conductance modulation by applied force

As shown as the black arrows in figure 1(c), the force is applied in the axial direction of nanotubes and to all carbon atoms of CNTs. The effect of applied force in the axial direction on thermal conductance is investigated with overlap lengths of 1.966 nm, 3.934 nm and 5.902 nm. Besides, the applied force is below the breaking force which is defined as the minimum force that can cut off the covalent bonds between CNTs totally and separate the two CNTs. As shown as the inserted image in figure 4, the CNTs junction is destroyed when the applied force is beyond breaking force. The positive dependence of breaking force on overlap length Δx is shown in figure 4. It is obvious that more covalent bonds contribute to CNTs junction with longer overlap length Δx, thus larger breaking force is needed to destroy the structure.

The thermal conductance as a function of applied force for overlap lengths of 1.966 nm, 3.934 nm and 5.902 nm is shown in figure 5. It is found that the thermal conductance is increased first and then decreased for the three cases. The thermal conductance G for overlap length of 1.966 nm is increased first from 2.81 to 3.42 nW K^{-1} as applied force is increased from 0 to 0.016 eV $Å^{-1}$ and decreased then from 3.42 to 1.88 nW K^{-1} as applied force is increased from 0.016 to 0.03 eV $Å^{-1}$ as shown in figure 5(a). The dependence of thermal conductance on applied force for overlap lengths of 1.966 nm, 3.934 nm and 5.902 nm is similar. The relationships between normalized thermal conductance (defined as the

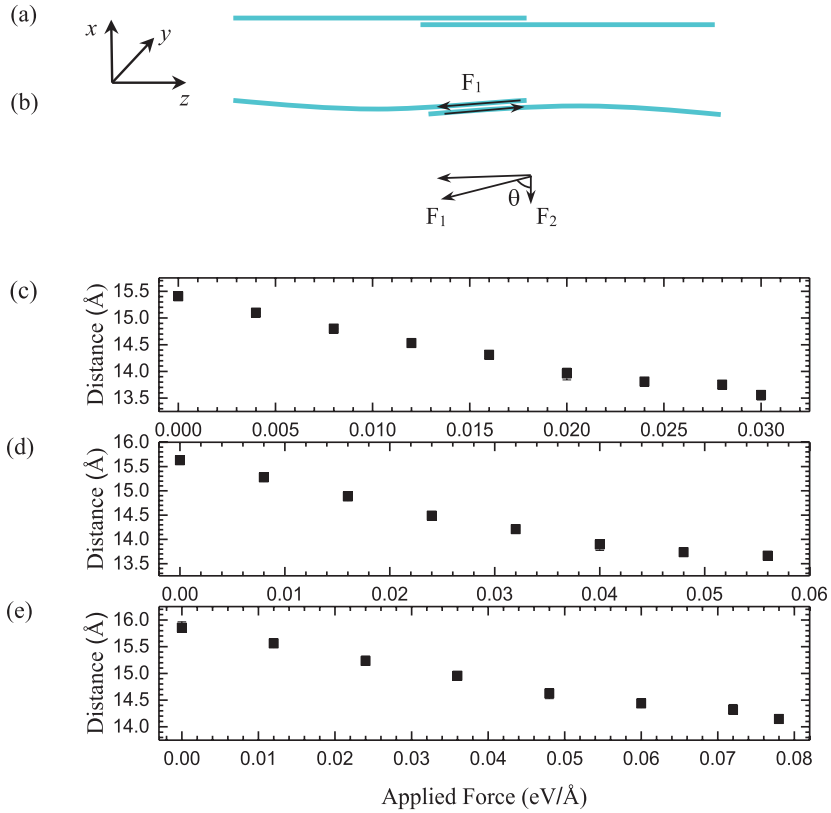

Figure 6. (a) The simplified initial structure of two bonded CNTs with overlap length of 3.934 nm. (b) The simplified structure of two bonded CNTs with overlap length of 3.934 nm under applied force. The CNTs become bent under applied force and the force F_1 along axis of CNT comes into being. The component force F_2 in x direction is decomposed from F_1 which equals to $F_1\cos\theta$. And the component force in the opposite direction in the other CNT is also decomposed. (c)–(e) The distance between CNTs at overlap segments as a function of applied force for overlap lengths of (a) 1.966 nm, (b) 3.934 nm and (c) 5.902 nm, and the distance between CNTs at overlap segments has an inverted dependence on applied force for three cases.

ratio of thermal conductance to the maximum value) and normalized applied force (defined as the ratio of applied force to corresponding value of overlap length) for overlap lengths of 1.966 nm, 3.934 nm and 5.902 nm are compared in figure 5(d). The overall trend for all three cases is similar. The variation of normalized thermal conductance for overlap length of 1.966 nm is largest, while that for overlap length of 5.902 nm is smallest. For the case of shorter overlap length, the ratio of number of cutting off bonds (as the applied force approaches breaking force) to the initial total number of bonds (without applied force) is larger.

Actually, the effect of applied force on thermal conductance is twofold. On the one hand, the applied force which is outward in the axial direction (z direction as shown in figure 1(c)) has a tendency to separate the two CNTs in the z direction. As the applied force is increased, the overlap length is shorter and the covalent bonds between CNTs are broken gradually, thus the energy coupling at the junction is weaker. On the other hand, the applied force causes deformation of CNTs, resulting in tangential force on CNTs. As shown as in figure 6(b), the CNTs become bent under the applied force and the force F_1 along the axis of CNT is generated. The component force F_2 in the x direction is decomposed from F_1 as $F_1 \cdot \cos\theta$. The opposed component force in the other CNT is also decomposed. The component force on the two CNTs squeezes CNTs. Thus, we found that the distance between CNTs which is calculated as the difference between average values of the x coordinates of all carbon atoms from two CNTs at the overlap segments is shorter during the simulation.

The distance between CNTs at overlap regime with different forces for overlap lengths of 1.966 nm, 3.934 nm and 5.902 nm is shown as figures 6(c)–(e), and the distance between CNTs at overlap regime has an inverted dependence on applied force for three cases. Increased applied force leads to more deformation on CNTs. Thus, the force F_1 as shown in figure 6(b) along the nanotube is increased and the angle θ between force F_1 and component force F_2 is increased for bent CNTs, resulting in increased F_2 which equals to $F_1 \cdot \cos\theta$. It is found that the distance between CNTs at the overlap regime is decreased with increasing F_2, leading to an inverse relationship of distance between CNTs and applied force. The closer CNTs at the overlap regime results in stronger interaction between them and improved heat transport at the junction.

As above-mentioned, the applied force has twofold effects on thermal transport. At the initial period, as the applied force is increased, the covalent bonds between CNTs are hardly cut off and the overlap length is decreased a little, while the distance between CNTs is decreased. The effect of spaced distance between CNTs dominates the thermal transport process, that is, the positive effect on thermal conductance. When the applied force is large enough (close to the breaking force), the covalent bonds between CNTs are broken significantly

as the forced is increased. Even if the CNTs become closer, destroyed covalent bonds will lead to an overall negative effect on thermal transport. That is why the thermal conductance between CNTs is increased first and then decreased as the applied force is increased.

In previous work, Yue *et al* [24] implemented thermal manipulation of CNT fiber by mechanical stretching and the thermal conductivity of CNT fiber improved as high as 28% with applied mechanical stretching less than 5% in the axial direction. It was explained that mechanical stretching could effectively improve the alignment of CNT fiber and the internal force gave pressure on CNT contacts, which improved thermal conductance between CNTs. It is noticed that the mechanical stretching applies force in the axial direction on CNT fiber and the most CNT contacts are applied with force in the axial direction since most CNTs are configured lengthways in CNT fiber. Thus, the most microstructures in CNT fiber with mechanical stretching are similar as the configuration in our work. The result in our work about effect of applied force on thermal conductance is complementary explanation to the thermal conductivity enhancement of CNT fiber with applied mechanical stretching from the micro level. Accordingly, the result in our work is reasonable and reliable with the experimental result [24].

4. Conclusions

Thermal transport between bonded and non-bonded CNTs are simulated for various overlap lengths, van der Waals interaction strength and applied force. The thermal conductance at the junction of two bonded CNTs is increased as the overlap length is increased and the thermal conductance per unit overlap length is also increased with overlap length. Thermal transport between two non-bonded CNTs is investigated by tuning van der Waals interaction scale factor for comparison with that of the bonded CNTs. The breaking force which is defined as the minimum force that can destroy the covalent bonds between CNTs is obtained with various overlap lengths. It is found that the distance between CNTs at overlap regimes is decreased with applied force, enhancing thermal transport. However, the covalent bonds between CNTs can be destroyed if applied force is too strong. We observe that the thermal conductance between CNTs is increased first and then decreased with applied force.

Acknowledgments

The financial support from the National Natural Science Foundation of China (No. 51576145) is gratefully acknowledged.

ORCID iDs

Jingchao Zhang https://orcid.org/0000-0001-5289-6062
Yanan Yue https://orcid.org/0000-0002-3489-3949

References

[1] Fujii M, Zhang X, Xie H, Ago H, Takahashi K, Ikuta T, Abe H and Shimizu T 2005 Measuring the thermal conductivity of a single carbon nanotube *Phys. Rev. Lett.* **95** 5502–5
[2] Berber S, Kwon Y K and Tomanek D 2000 Unusually high thermal conductivity of carbon nanotubes *Phys. Rev. Lett.* **84** 4613–6
[3] Zhang H L, Li J F, Yao K F and Chen L D 2005 Spark plasma sintering and thermal conductivity of carbon nanotube bulk materials *J. Appl. Phys.* **97** 4310–4
[4] Han Z and Fina A 2011 Thermal conductivity of carbon nanotubes and their polymer nanocomposites: a review *Prog. Polym. Sci.* **36** 914–44
[5] Moisala A, Li Q, Kinloch I A and Windle A H 2006 Thermal and electrical conductivity of single- and multi-walled carbon nanotube-epoxy composites *Compos. Sci. Technol.* **66** 1285–8
[6] Aliev A E, Lima M H, Silverman E M and Baughman R H 2010 Thermal conductivity of multi-walled carbon nanotube sheets: radiation losses and quenching of phonon modes *Nanotechnology* **21** 5709–19
[7] Bui K, Grady B P and Papavassiliou D V 2011 Heat transfer in high volume fraction CNT nanocomposites: effects of inter-nanotube thermal resistance *Chem. Phys. Lett.* **508** 248–51
[8] Vallabhaneni A K, Qiu B, Hu J, Chen Y P, Roy A K and Ruan X 2013 Interfacial thermal conductance limit and thermal rectification across vertical carbon nanotube/graphene nanoribbon-silicon interfaces *J. Appl. Phys.* **113** 4311–6
[9] Li C, Xu S, Yue Y, Yang B and Wang X 2016 Thermal characterization of carbon nanotube fiber by time-domain differential Raman *Carbon* **103** 101–08
[10] Li M, Li C, Wang J, Xiao X and Yue Y 2015 Parallel measurement of conductive and convective thermal transport of micro/nanowires based on Raman mapping *Appl. Phys. Lett.* **106** 253108
[11] Yue Y, Zhang J, Xie Y, Chen W and Wang X 2017 Energy coupling across low-dimensional contact interfaces at the atomic scale *Int. J. Heat Mass Transfer* **110** 827–44
[12] Hu L and McGaughey A J 2014 Thermal conductance of the junction between single-walled carbon nanotubes *Appl. Phys. Lett.* **105** 310–4
[13] Hu G J and Cao B Y 2013 Thermal resistance between crossed carbon nanotubes: molecular dynamics simulations and analytical modeling *J. Appl. Phys.* **114** 430–8
[14] Varshney V, Patnaik S S, Roy A K and Farmer B L 2010 Modeling of thermal conductance at transverse CNT–CNT interfaces *J. Phys. Chem.* C **114** 16223–8
[15] Yang J, Waltermire S, Chen Y, Zinn A A, Xu T T and Li D 2010 Contact thermal resistance between individual multiwall carbon nanotubes *Appl. Phys. Lett.* **96** 3109–11
[16] Volkov A N, Salaway R N and Zhigilei L V 2013 Atomistic simulations, mesoscopic modeling, and theoretical analysis of thermal conductivity of bundles composed of carbon nanotubes *J. Appl. Phys.* **114** 4301–21
[17] Xu Z and Buehler M J 2009 Nanoengineering heat transfer performance at carbon nanotube interfaces *ACS Nano* **3** 2767–75
[18] Salaway R N and Zhigilei L V 2016 Thermal conductance of carbon nanotube contacts: molecular dynamics simulations and general description of the contact conductance *Phys. Rev.* B **94** 4308–24
[19] Zhong H and Lukes J R 2006 Interfacial thermal resistance between carbon nanotubes: molecular dynamics simulations and analytical thermal modeling *Phys. Rev.* B **74** 5403–12

[20] Shao C, Yu X, Yang N, Yue Y and Bao H 2017 A review of thermal transport in low-dimensional materials under external perturbation: effect of strain, substrate, and clustering *Nanoscale Microscale Thermophys. Eng.* **21** 1–36
[21] Evans W J, Shen M and Keblinski P 2012 Inter-tube thermal conductance in carbon nanotubes arrays and bundles: effects of contact area and pressure *Appl. Phys. Lett.* **100** 1908–11
[22] Chen W, Zhang J and Yue Y 2016 Molecular dynamics study on thermal transport at carbon nanotube interface junctions: effects of mechanical force and chemical functionalization *Int. J. Heat Mass Transfer* **103** 1058–64
[23] Liu G, Huang X, Wang Y, Zhang Y-Q and Wang X 2012 Thermal transport in single silkworm silks and the behavior under stretching *Soft Matter* **8** 9792–9
[24] Yue Y, Liu K, Li M and Hu X 2014 Thermal manipulation of carbon nanotube fiber by mechanical stretching *Carbon* **77** 973–9
[25] Plimpton S 1995 Fast parallel algorithms for short-range molecular dynamics *J. Comput. Phys.* **117** 1–19
[26] Hoover W 1983 Nonequilibrium molecular dynamics *Ann. Rev. Phys. Chem.* **34** 103–27
[27] Stuart S J, Tutein A B and Harrison J A 2000 A reactive potential for hydrocarbons with intermolecular interactions *J. Chem. Phys.* **112** 6472–86
[28] Saito R, Matsuo R, Kimura T, Dresselhaus G and Dresselhaus M 2001 Anomalous potential barrier of double-wall carbon nanotube *Chem. Phys. Lett.* **348** 187–93
[29] Zhang J, Hong Y and Yue Y 2015 Thermal transport across graphene and single layer hexagonal boron nitride *J. Appl. Phys.* **117** 430–7
[30] Shi J, Dong Y, Fisher T and Ruan X 2015 Thermal transport across carbon nanotube-graphene covalent and van der Waals junctions *J. Appl. Phys.* **118** 044302
[31] Evans D J and Holian B L 1985 The Nose–Hoover thermostat *J. Chem. Phys.* **83** 4069–74
[32] Yang X, Chen D, Han Z, Ma X and To A C 2014 Effects of welding on thermal conductivity of randomly oriented carbon nanotube networks *Int. J. Heat and Mass Transfer* **70** 803–10
[33] Frank O, Tsoukleri G, Parthenios J, Papagelis K, Riaz I and Jalil R 2010 Compression behavior of single-layer graphenes *ACS Nano* **4** 3131–8
[34] Wei N, Xu L, Wang H Q and Zheng J C 2011 Strain engineering of thermal conductivity in graphene sheets and nanoribbons: a demonstration of magic flexibility *Nanotechnology* **22** 105705
[35] Cui L, Du X, Wei G and Feng Y 2016 Thermal conductivity of graphene wrinkles: a molecular dynamics simulation *J. Phys. Chem.* C **120** 23807–12
[36] Schiffres S N, Kim K H, Hu L, McGaughey A J, Islam M F and Malen J A 2012 Gas Diffusion, energy transport, and thermal accommodation in single-walled carbon nanotube aerogels *Adv. Funct. Mater.* **22** 5251–8
[37] Sun L, Banhart F, Krasheninnikov A, Rodriguez-Manzo J, Terrones M and Ajayan P 2006 Carbon nanotubes as high-pressure cylinders and nanoextruders *Science* **312** 1199–202
[38] Hu M, Keblinski P, Wang J-S and Raravikar N 2008 Interfacial thermal conductance between silicon and a vertical carbon nanotube *J. Appl. Phys.* **104** 350–3